Journal of Nepal Geological Society, 2001, Vol. 23, pp. 71–78

Estimation of source parameters and depth of focus of the earthquake of Sikkim Himalaya by waveform modelling

K. N. Khanal
Central Department of Physics, Tribhuvan University, Kirtipur, Kathmandu, Nepal

ABSTRACT

The earthquake of 19 November 1980, which occurred in the Sikkim Himalaya was investigated by waveform modelling technique. The synthetic seismograms for both the P- and S-waves were generated using wave number integration method. The P- wave seismograms were generated using different velocity models for the source and receiver crusts. The S-wave seismograms were produced using only the half-space model for both the source and receiver crusts. Comparing the seismograms of these waves with the respective seismograms digitally recorded by the Global Digital Seismograph Network the source parameters have been estimated. The orientation parameters determined in this way are strike = 119°, dip = 74° and dip direction = S29W for one modal plane and strike = 218°, dip= 64° and dip direction = N52W for the other modal plane. The modal plane striking in NW direction has been preferred as representing the fault plane. The depth of the earthquake has been estimated to be 22 km. The total duration of the rupture process has been estimated to be 7 s.

INTRODUCTION

The analysis of fault-plane solutions and depth of focus of earthquakes can throw light on the active tectonics of a region. Many investigators have therefore addressed this problem by studying the earthquakes in the Himalaya (e.g., Seeber et al. 1981; Khattri and Tyagi 1983b; Baranowski et al. 1984; Molnar 1984; Ni and Barazangi 1984; Seeber and Armbruster 1984; Das Gupta et a1.1987; Khattri et a1.1989; Ni 1989).

The techniques used in order to determine the fault-plane solutions of earthquakes range from the use of the first motion of P-waves to the waveform modelling of P- and S-waves. The waveform modelling technique utilises a larger part of the information available in seismograms as compared to that utilised in the first motion method. The waveform modelling technique also allows constraining the depth of focus.

The waveform modelling technique requires the calculation of synthetic seismograms for suitable model of earthquake and the medium. The displacement caused by an earthquake is expressed in terms of a dislocation source, which is in the form of a double integral, one over the wave number and the other over the frequency. One way to evaluate this double integral is to evaluate first the wave number integral and next the frequency integral. This is called the wave number integration method (e.g., Fuchs and Müller 1971; Herrmann 1978; Barker 1984; Müller 1985, Herrmann and Wang 1985).

In the present investigation, the earthquake of 19 November 1980 was studied by modelling both the teleseismic P- and S-waves. The observed seismograms recorded by the Global Digital Seismograph Network (GDSN) were used. The orientation parameters were strike, dip, and slip. The source–time function together with the depth of focus of the earthquake was estimated by matching synthetic seismograms with the observed ones. The fault-plane solution obtained in this way is considered in the light of the tectonics of the region.

GEOLOGY AND TECTONICS

The main tectonic features of the region are shown in Fig. 1. The Indus–Tsangpo Suture (ITS) separates the Trans-Himalaya in the north and the Tethys Himalaya in the south. The Great Himalaya lies just south of the Tethys Himalaya and consists of crystalline rocks. The Main Central Thrust (MCT) separates the Great Himalaya from the Lesser Himalaya. The Main Boundary Thrust (MBT) separates the Lesser Himalaya (composed of sedimentary and metasedimentary rocks) from the Siwaliks (composed of molassic deposits) in the south. The Siwaliks are separated from the Gangetic fore deep by the Main Frontal Thrust (MFT).

Many active transverse tectonic features are also present in this region (Valdiya 1976, 1998; Khattri and Tyagi 1983a; Das Gupta et a1. 1987; Verma and Krishna Kumar 1987).

THEORY

The medium is considered to be composed of the source crust, mantle, and receiver crust. The source and receiver crusts are represented by laterally homogeneous isotropic layers with N^{th} layer as a half space and each layer defined by P-wave velocity (Vp), S-wave velocity (Vs), density (d), and thickness (thk). The mantle is represented by a medium with a prescribed velocity function and attenuation properties (Langston and Helmberger 1975).

The source was represented by a displacement dislocation (Fig. 2), which is present in one of the layers in

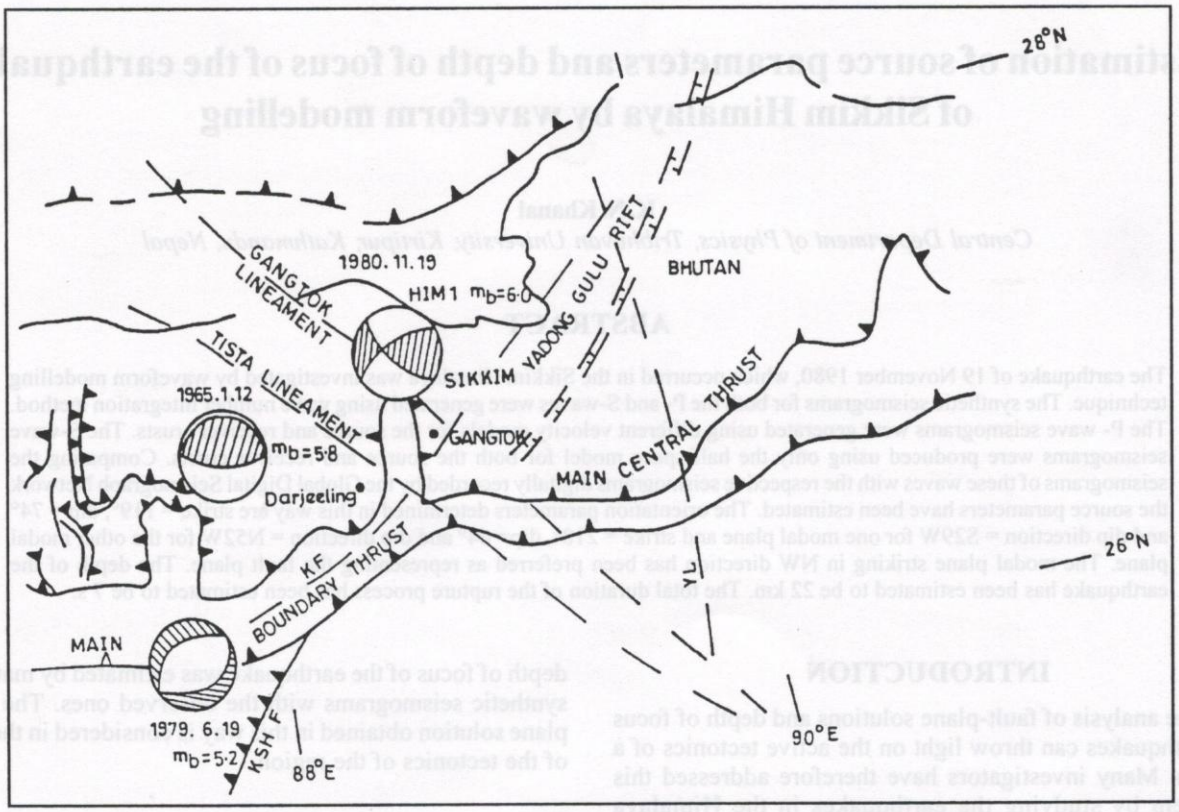

Fig. 1: Map showing the location of the earthquake. KF - Kanchanjunga fault, KSH F - Kishangunj fault, YL-Yamuna Lineament (after Gansser 1964; Searle et al. 1987)

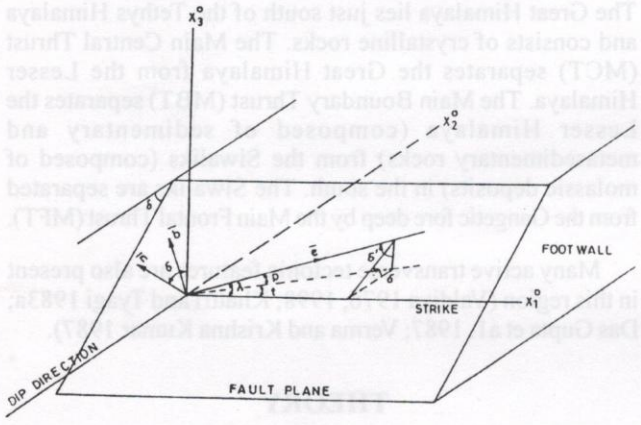

Fig. 2: The representation of the earthquake in terms of the fault geometry and the slip orientation. λ=slip angle, δ=dip, p=plunge, t=trend, ē=unit slip vector, n̄=normal, and b̄= null vector.

the source crust. The waves propagated from the source pass through the crust–mantle–crust path (Fig. 3) and they are recorded at the stations. Using the condition of continuity of stress-motion vector (except at the source), the displacements caused by the earthquake are calculated.

As seismograms are the output of the source–medium–instrument system (which is treated to be linear), the synthetic seismogram r(t) is given by the convolutional output of the following components (Herrmann 1976; Helmberger and Burdick 1979; Barley and Pearce 1977).

$$r(t) = s(t)^* h_{sc}(t)^* h_m(t)^* h_{rc}(t)^* h_i(t)$$

where t is the time, s(t) is the seismic radiation from the source, $h_{sc}(t)$ and $h_{rc}(t)$ are the impulse responses of the source and the receiver crusts respectively, $h_m(t)$ is the mantle response, $h_i(t)$ is the impulse response of the instrument, and * is the convolution operator.

The source is specified in terms of scalar seismic moment, orientation angles (viz., strike, dip, and slip of the fault), depth of focus, and source–time function s(t). The source–crust transfer function was evaluated by the propagator matrix method (Haskell 1964; Gilbert and Backus 1966; Hudson 1969a,b). The mantle response consists of the effects of attenuation and geometrical divergence (Langston and Helmberger 1975). The receiver crust transfer function has been evaluated by Haskell matrix method (Haskell 1953). The transfer function of the appropriate instrument system was used.

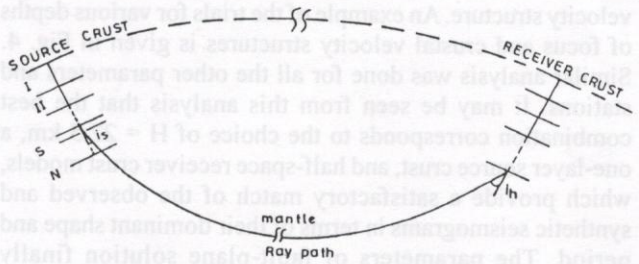

Fig. 3: Source - medium geometry

ANALYSIS

The analysis of seismograms was carried out by the following procedure.

Source Parameters

The scalar seismic moment that represents the strength of the source was used as a multiplicative factor. The orientation parameters, source–time function, and depth of focus of the source were estimated by trial and error. The initial estimate of source–time function was made on the basis of the magnitude of earthquake.

Medium parameters

The velocity models used in this investigation are based on the work of Kaminuma (1964), Barazangi and Ni (1982), Ni and Barazangi (1983), and Lyon-Caen (1986). These models are given in Table 1. The attenuation in the mantle were expressed in terms of the quality factor Q and travel time T as T/Q. T/Q was taken as 1 for P-waves and 3 for S-waves as a reasonable approximation at teleseismic distances between 30° and 90° (Langston and Helmberger 1975).

Station parameters

The epicentral distance, azimuth, and back azimuth were determined using spherically symmetric earth (Richter 1958). The take-off angles were obtained from the table of Pho and Behe (1972). The phase velocities were determined by using the relation: $c = V_p / \text{Sin}\,(i_h)$, where V_p is the P-wave velocity and i_h is the take-off angle of the ray at the source. The S-wave velocity V_s was estimated from V_p assuming a Poisson's ratio of 0.25. All these parameters are given in Table 2. A sampling rate of 0.5 s was used in order to generate the synthetic seismograms.

OBSERVED SEISMOGRAMS

The GDSN that started operation in the early seventies has become the source of high-quality digital data. The United States Geological Survey (USGS) collects these data from all these stations and distributes them in the form of the Network-Day Tapes (NDTs) or the Event Tapes (ETs). The NDT consists of data recorded in 26 hours (including two hours of the next day) in order to record the event of the day completely. The ET consists of the data of some selected events. The format of both of these tapes is same. Apart from the data portion (i.e., digital seismograms) the information about the source, stations, and instrument transfer function together with the sampling rate are stored in appropriate locations in the tapes (Hoffman 1980; Peterson et a1.1980). The data used in the present investigation were extracted from the NDTs. A software package that was used to retrieve data as well as other necessary information from these tapes is also available from the USGS (Zirbes and Bul and 1981).

In the present investigation, the long period P- and S-waves were used for source study. The arrival times of the waves at different stations were calculated using the J-B

Table 1: Velocity models for the source and the receiver crusts

	Source crust				Receiver crust			
	Thk (km)	Vp (km/s)	Vs (km/s)	d (gm/cc)	Thk (km)	Vp (km/s)	Vs (km/s)	d (gm/cc)
Model (a)	--	6.0	3.45	2.7	--	6.0	3.45	2.7
Model (b)	60	6.2	3.7	2.7	--	--	--	--
	--	8.2	4.82	3.3	--	6.0	3.45	2.7
Model (cl	60	6.2	3.7	2.7	33	6.5	3.81	2.7
	--	8.2	4.82	3.3	--	8.2	4.82	3.3

Table 2: The parameters of the stations for the earthquake

Code no.	Station	Delta (deg)	Azimuth (deg)	Back Azimuth (deg)	c (km/s)	i_h (deg)
31	ANTO	47.44	300.29	92.69	12.7	28.2
35	GUMO	53.90	92.89	294.18	13.5	26.3
39	GRFO	61.65	314.13	99.91	14.6	24.3
41	TATO	29.39	87.18	281.96	11.1	32.8
50	CTAO	73.14	124.14	308.52	16.7	21.1
53	MAJO	42.47	64.72	267.79	12.1	29.6
54	KONO	61.22	325.51	95.78	14.6	24.4

tables (Jeffereys and Bullen 1940). Since we were interested in the P- and S-wave seismograms, the data in 5-minute window placed about 1 minute prior to the arrival times of P- and S-waves, respectively, were extracted.

RESULTS

The hypocentral parameters of the investigated earthquake are given in Table 3. The fault-plane solution is obtained by trying out various combinations of strike, dip, pitch, source–time function, depth of focus, and crustal velocity structure. An example of the trials for various depths of focus and crustal velocity structures is given in Fig. 4. Similar analysis was done for all the other parameters and stations. It may be seen from this analysis that the best combination corresponds to the choice of H = 22.5 km, a one-layer source crust, and half-space receiver crust models, which provide a satisfactory match of the observed and synthetic seismograms in terms of their dominant shape and period. The parameters of fault-plane solution finally obtained in this way are given in Table 4. Fig. 5 shows the

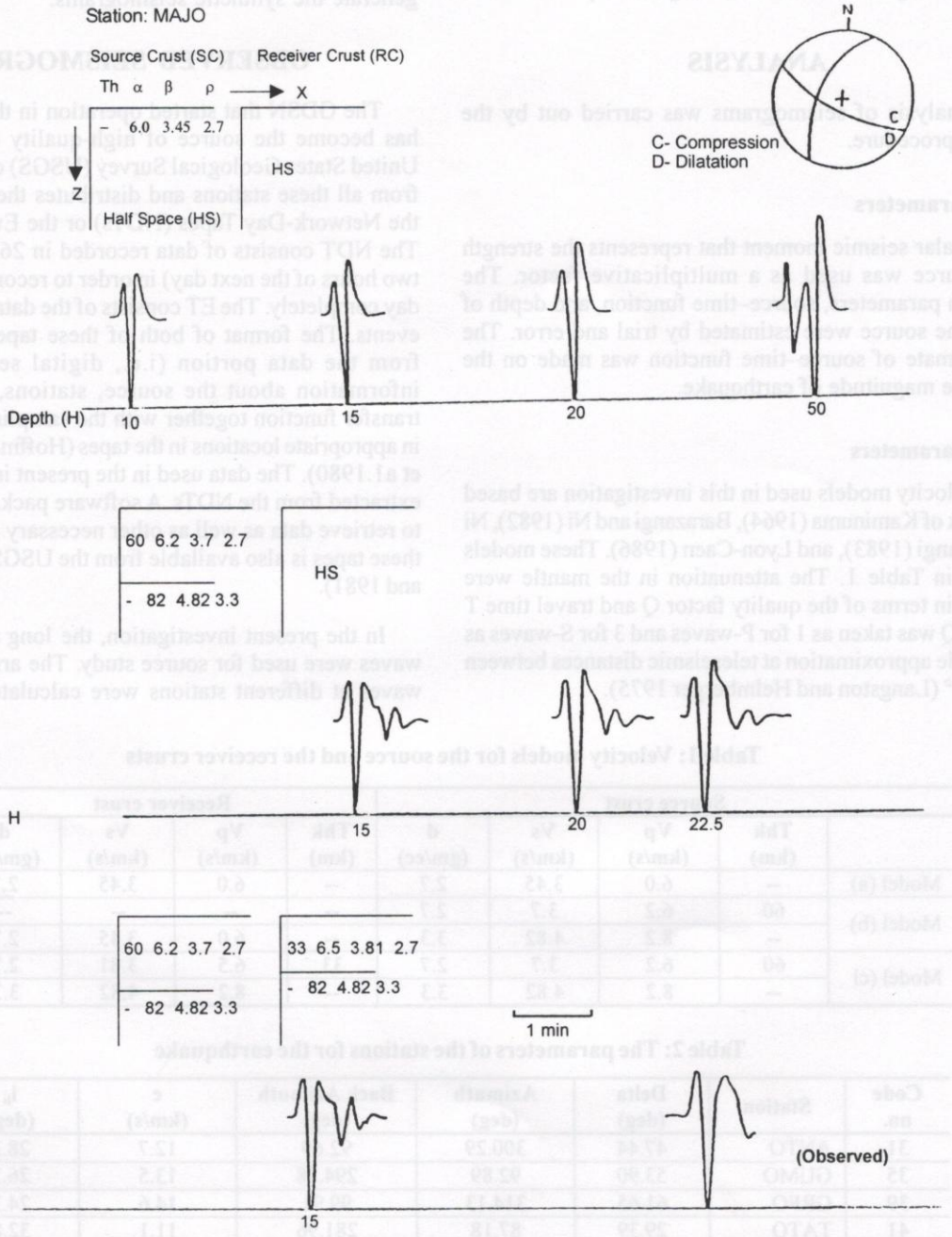

Fig. 4: The synthetic seismograms generated at the station MAJO using different velocity models for the source and the receiver crusts. The wave velocities Vp and Vs are expressed in km/s, the density (d) in gm/cc, the depth of focus (H) and the thickness of the layer (Thk) are in km.

fault-plane solution of the earthquake along with the observed and synthetic seismograms. The solution shows dominantly strike-slip faulting.

The observed long-period S-wave seismograms were noisy. Two examples are shown in Fig. 6. The smoothed S-waveforms abstracted from the observed seismograms are also shown. It was decided to model them using a half-space model for the source as well as the receiver crusts and the source model obtained using the P-waves.

Fig. 7 shows the fault-plane solution and the smoothed observed S-waveforms along with the synthetic S-wave seismograms. The match is fair for stations KONO, GRFO, and CTAO and is not satisfactory for the remaining ones.

We note that the earthquake under investigation was also analysed by Ni and Barazangi (1984) and Das Gupta et al. (1987), and they also found fault-plane solutions very similar to the one obtained by us.

Table 3: The hypocentral parameters and the magnitudes of the earthquake analysed

Year	Mo	Da	Hr	Mn	Secs	Lat. (N) (deg)	Long. (E) (deg)	Depth (km)	mb	Ms
1980	11	19	19	00	46.9	27.394	88.752	17.0	6.0	6.1

Table 4: Source parameters of the earthquake determined in the study

Fault plane			Focal depth (km)	Duration of the source time function (Secs)	Body wave magnitude (mb)
Strike (deg)	Dip (deg)	Slip (deg)			
119	74	85	22	7	6.0

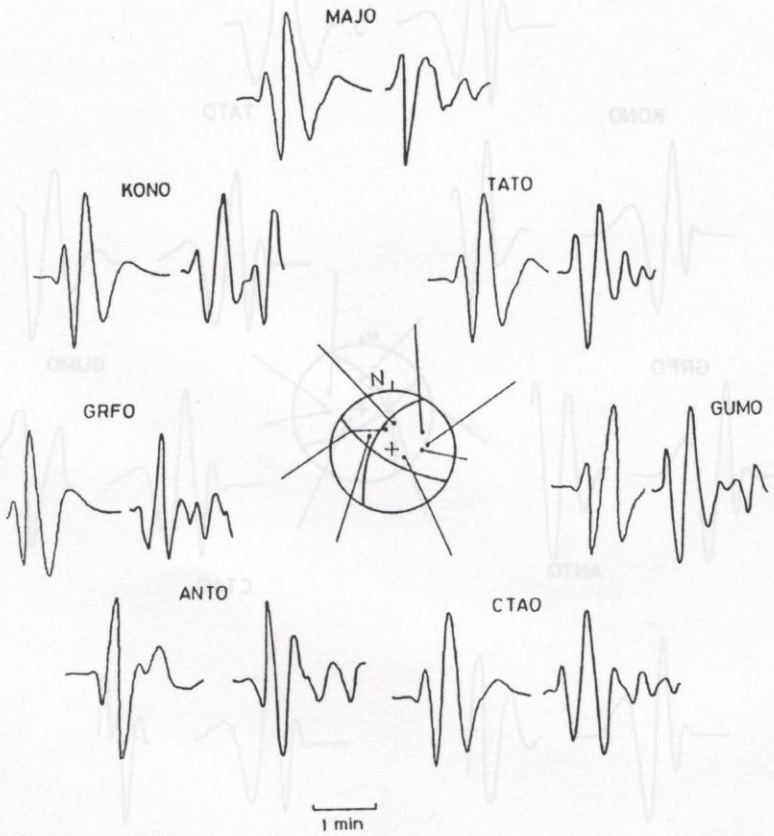

Fig. 5: The fault-plane solution of the earthquake determined by waveform modelling together with the synthetic (left) and the observed (right) P-wave seismograms. MAJO: Matsushire, Japan; KONO: Kongsbarg, Finland; TATO: Taipei, Taiwan; GRFO: Grafenberg, Germany; GUMO: Guam, Merina Island; ANTO: Ankara, Turkey; CTAO: Charter Tower, Australia

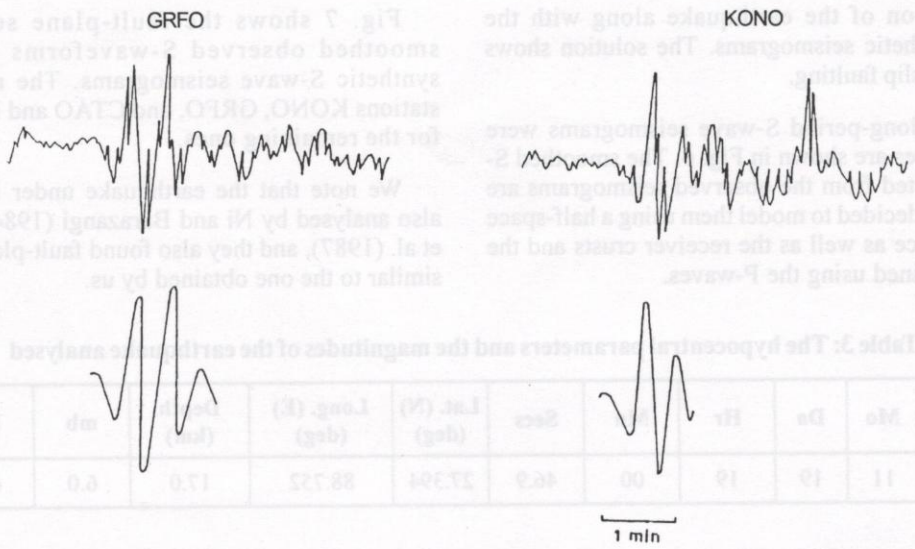

Fig. 6: The noisy S-wave observed seismograms of the stations GRFO and KONO. The smoothed seismograms are also shown below them.

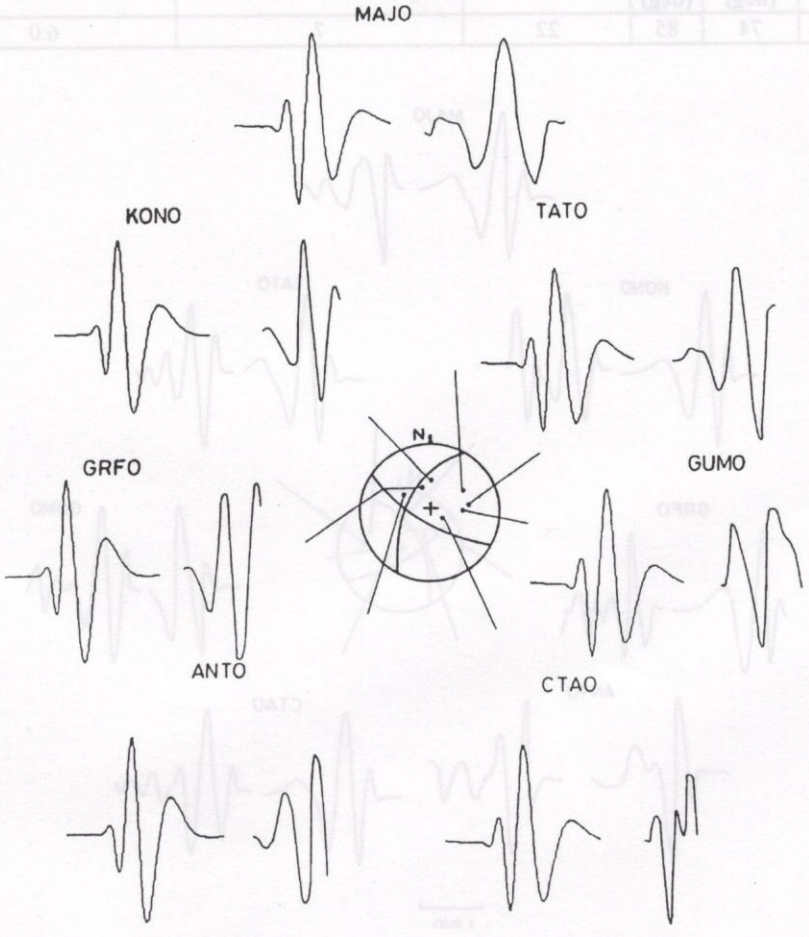

Fig. 7: The synthetic (left) as well as the observed (right) seismograms of the S-waves from the preferred fault-plane solution obtained from P-wave modelling (see Fig. 5 for abbreviations).

CONCLUSIONS AND DISCUSSIONS

The following general conclusions were derived from the simulation experiments.

1. While estimating the orientation parameters by trial-and-error method, it has been found that the change of any one of the orientation parameters viz., strike, dip, and slip by up to about 10° does not show any remarkable difference in the form of seismograms.
2. The periods of P- and S-waves are positively correlated with the duration of source–time function. This was also concluded by other workers (viz., Hatanaka and Shimazaki 1988; Khanal et al. 1989).
3. The depth of focus is also positively correlated with the dominant period of waves. Thus, there will be a trade off between the depth of focus and the source–time function while estimating these two parameters (Christensen and Ruff 1985; Wagner and Langston 1989; Khanal et al. 1989). This ambiguity has to be resolved with the help of external information such as the time difference between the pP- and P-waves and the like.

The matching of the synthetic and the observed seismogram for the earthquake analysed here are in fair agreement in term of their overall shapes and dominant periods. There are differences when one looks at the details of the waveforms, which might be due to inadequate velocity models used in the present investigation and other simplifying assumptions made.

This earthquake was also studied by Ni and Barazangi (1984) using Waveform Modelling Technique. Their solution is close to ours. However, the depth of focus obtained by them was 13± 4 km as compared to 22 km estimated here. The depth of focus given by the USGS (Zirbes and Buland 1981) was 17 km, whereas it was calculated as 47 km in the International Seismological Summary (Das Gupta et al. 1987). We believe that the actual depth of focus lies in the range of the depth estimates obtained by waveform modelling. The first motion study also gives a similar fault-plane solution (Das Gupta et al. 1987).

On the basis of the location of epicentre of earthquake, we assume that the earthquake was related to the tectonic activity along the Gangtok lineament. If this interpretation is correct, then right-lateral strike-slip faulting may have occurred along the fault plane that is trending in the northwest direction parallel to the lineament.

The strike-slip mechanism may be explained in terms of the switching of directions of intermediate and least principal stress axes in a compressive (σ_1 in N–S direction and sub-horizontal) stress regime of the Himalayan collision zone. However, the normal faulting, which occurred close to the MBT, requires at least locally an extensional stress regime for the origin of which a suitable model is needed.

ACKNOWLEDGEMENTS

This work was supported by the Department of Earth Sciences, University of Roorkee and the Department of Science and Technology, Government of India, New Delhi. Tribhuvan University granted leave to the author.

REFERENCES

Baranowski, J., Armbruster, J., Seeber, L., and Molnar, P., 1984, Focal depths and fault-plane solutions of earthquakes and active tectonics of the Himalaya. Jour. Geophys. Res., v. 89, pp. 6918–6928.

Barazangi, M. and Ni, J., 1982, Velocities and propagation Characteristics of Pn and Sn beneath the Himalayan arc and the Tibetan plateau: Possible evidence of underthrusting of Indian continental lithosphere beneath Tibet. Geology, v. 10, pp. 179–185.

Barker, J., 1984, A seismological analysis of the May 1980 Mammoth Lakes, California earthquakes. Ph. D. Thesis, Pennsylvania State University.

Barley, B. J. and Pearce, R. G., 1977, A fault-plane solution using theoretical P-seismograms. Geophys. Jour. R. A. Soc., v. 51, pp. 653–668.

Christensen, D. H. and Ruff, L. J., 1985, Analysis of the trade off between hypocentral depth and source–time function. Bull. Seis. Soc. Am., v. 75, pp. 1637–1656.

Das Gupta, S., Mukhopadhyay, M., and Nandy, D. R., 1987, Active transverse features of the central portion of the Himalaya. Tectonophysics, v. 136, pp. 255–264.

Fuchs, K. and Müller, G., 1971, Computation of synthetic seismograms with the reflectivity method and comparison with observations. Geophys. Jour. R. A. Soc., v. 23, pp. 417–433.

Gansser, A., 1964, *Geology of the Himalaya*. Inter Science, New York, 298 p.

Gilbert, F. and Backus, G. E., 1966, Propagator matrices in elastic wave and vibration problems. Geophysics, v. 31, pp. 326–332.

Haskell, N. A., 1953, The dispersion of surface wave on multilayered media, Bull. Seis. Soc. Ame., v. 43, pp. 17–34.

Haskell, N. A., 1964, Radiation pattern of surface waves from point sources in a multilayered medium. Bull. Seis. Soc. Am., v. 54, pp. 377–393.

Hatanaka, Y. and Shimazaki, K., 1988, Rupture processes of the 1975 central Oita, Japan earthquake. Jour. Phy. Earth, v. 36, pp. 1–15.

Helmberger, D. V. and Burdick, L. J., 1979, Synthetic Seismograms. Ann. Rev. Ear. Planet. Sci., v. 7, pp. 417–442.

Herrmann, R. B., 1976, Focal depth determination from the signal character of long period P-waves. Bull. Seis. Soc. Ame., v. 66, pp. 1221–1232.

Herrmann, R. B., 1978, Computer program in earthquake seismology. v. 1, Report, Saint Louis University, USA.

Herrmann, R. B. and Wang, C. Y., 1985, A comparison of synthetic seismograms. Bu11. Seis. Soc. Am., v. 75, pp. 41–56.

Hoffman, J. P., 1980, The global digital seismograph network-day tape. Open file report 80-289, USGS.

Hudson, J. A., 1969a, A quantitative evaluation of seismic signals at teleseismic distances: I. Radiation from point sources. Geophys. Jour. R. A. Soc., v. 18, pp. 233–249.

Hudson, J. A., 1969b, A quantitative evaluation of seismic signals at teleseismic distances: II. Body waves and surface waves from an extended source. Geophys. Jour. R. A. Soc., v. 18, pp. 353–370.

Jeffereys, H. and Bullen, K. E., 1940, Seismological Tables.

Kaminuma, K., 1964, Crustal structure in Japan from the phase velocity of Rayleigh waves: Part 3. Rayleigh waves from the Mindanao shock of September 24, 1957, Bull. Eq. Res. Inst., Tokyo Univ., v. 42, pp. 19–38.

Khanal, K. N., Khattri, K. N., Chander, R., and Singh, V. N., 1989, Estimation of source parameters and depth of focus of an earthquake of central Himalaya by waveform modelling using GDSN seismograms, seminar on earthquake process and their consequences: Seismological investigations. Department of Mathematics Kurukshetra University, India.

Khattri, K. N. and Tyagi, A. K., 1983a, Transverse tectonic features in the Himalaya. Tectonophysics, v. 96, pp. 19–29.

Khattri, K. N. and Tyagi, A. K., 1983b, Seismicity pattern in the Himalayan plate boundary and identification of the areas of high seismic potential. Tectonophysics, v. 96, pp. 281–297.

Khattri, K. N., Chander, R., Mukhopadhyay, S., Sri Ram, V., and Khanal, K. N., 1989, A model of the active tectonics of the Shillong massif region in Himalaya orogen and global tectonics (A. K. Sinha ed.). Oxford and IBH Pub. Co., New Delhi.

Langston, C. A. and Helmberger, D. V., 1975, A procedure for modelling shallow dislocation sources. Geophys. Jour. R. A. Soc., v. 42, pp. 117–130.

Lyon-Caen, H., 1986, Comparison of the upper mantle shear wave velocity structure of the Indian shield and Tibetan plateau and tectonic implications. Geophys. Jour. R. A. Soc., v. 86, pp. 727–749.

Molnar, P., 1984, Structure and tectonics of the Himalaya: constraints and implications of geophysical data. Ann. Rev. Earth Pla. Sci., v. 12, pp. 489–518.

Müller, G., 1985, The reflectivity method: a tuterial. Jour. Geophysics, v. 58, pp. 153–174.

Ni, J., 1989, Active tectonics of the Himalaya. Proc. Ind. Acad. Sci., v. 98, pp. 71–89.

Ni, J., and Barazangi, M., 1983, Velocities and propagation characteristics of Pn, Pg, Sn, and Sg seismic waves beneath the Indian shield, Himalayan arc, Tibetan plateau and surrounding regions: High uppermost mantle velocities and efficient Sn propagation beneath Tibet. Geophys. Jour., R. A. Soc., v. 73, pp. 665–689.

Ni, J. and Barazangi, M., 1984, Seismotectonics of the Himalayan collision zone: Geometry of the underthrusting Indian plate beneath the Himalaya. Jour. Geophys. Res., v. 89, pp. 1147–1163.

Peterson, J., Hutt, C. R., and Holcomb, L. G., 1980, The seismic research observatory. Open file report, pp. 80–187, VSGS.

Pho, H-T. and Behe, L., 1972, Extended distances and angle of incidence of P-waves. Bull. Seis. Soc. Ame., v. 62, pp. 885–902.

Richter, C. F., 1958, *Elementary Seismology*. W. H. Freeman and Co., San Francisco, 768 p.

Searle, M. P., Windley, B. F., Coward, M. P., Cooper, D. J. W., Rex, A. J., Rex, D., Tingdong, Li., Xuchang, Xiao, Jan, M. Q. Thakur, V. C., and Kumar, S., 1987, The closing of Tethys and the tectonics of the Himalaya. Geol. Soc. Ame. Bull., v. 98, pp. 678–701.

Seeber, L., Armbruster, J. G., and Quittmeyer, R. C., 1981, Seismicity and continental subduction in Himalayan arc, in Zagros Hindukush, Himalaya. In: H. K. Gupta and F. M. Delany (eds.), *Geodynamic evolution*. AGU, Washington D. C.,Geodyn. Ser. v. 3, pp. 215–242.

Seeber, L. and Armbruster, J. G., 1984, Some elements of continental subduction along the Himalayan front. Tectonophysics, v. 105, pp. 263–278.

Valdiya, K. S., 1976, Himalayan transverse faults and folds and their parallelism with subsurface structures of north Indian plains. Tectonophysics, v. 32, pp. 353–386.

Valdiya, K. S., 1998, *Dynamic Himalaya*. Universities Press (India) Limited, Hyderabad, India, 178 p.

Verma, R. K. and Krishna Kumar, G. V. R., 1987, Seismicity and the nature of plate movement along the Himalayan arc, North east India and Arakan Yoma: a review. Tectonophysics., v. 134, pp. 153–175.

Wagner, G. S. and Langston, C. A., 1989, Some pitfalls and trade offs in source parameter determination using body wave modelling and inversion. Tectonophysics, v. 166, pp. 101–114.

Zirbes, M. and Buland, R., 1981, Network-Day Tape software users guide. Open file report, pp. 81–666, USGS.